Analysis of the microcharacteristics of different kinds of asphalt based on different aging conditions

Pei, Zhongshi; Xu, Meng; Cao, Jiwei; Feng, Decheng; Hu, Wei; Ren, Junda; Jing, Ruxin; Yi, Junyan

DOI
10.1617/s11527-022-02088-3

Publication date
2022

Document Version
Final published version

Published in
Materials and Structures/Materiaux et Constructions

Materials and Structures (2022)55:250
https://doi.org/10.1617/s11527-022-02088-3

ORIGINAL ARTICLE

Analysis of the microcharacteristics of different kinds of asphalt based on different aging conditions

Zhongshi Pei · Meng Xu · Jiwei Cao · Decheng Feng · Wei Hu · Junda Ren · Ruxin Jing · Junyan Yi

Received: 27 June 2022 / Accepted: 2 December 2022

Abstract Asphalt aging often leads to rapid degradation of road performance, which seriously affects the service life of asphalt pavement. Exploring the influence of asphalt oil sources, asphalt grades, and filler types on asphalt microcharacteristics in the asphalt aging process can provide an essential reference to guide asphalt pavement maintenance. In this study, we selected seven kinds of asphalt and three fillers commonly used in China for research. The pressurized aging vessel (PAV) and homemade ultraviolet (UV) aging equipment were used to perform thermo-oxidative aging and UV aging tests, respectively, of asphalt. The microcharacteristics of asphalt before and after aging were analyzed via attenuated total reflectance fourier transformation infrared spectroscopy and nuclear magnetic resonance ^{1}H spectroscopy. The results show that the oil source of asphalt exerted the most significant influence on the microcharacteristics of the aged asphalt, while the effect of the asphalt grade was relatively limited. The addition of fillers did not affect the aging mechanism of asphalt. UV and PAV aging generated apparent differences in the changes in the aged asphalt microstructure.

Keywords Road materials · Oil source of asphalt · Grade of asphalt · Thermo-oxidative aging · Ultraviolet aging · Microcharacteristics

Z. Pei · D. Feng · J. Yi (✉)
School of Transportation Science and Engineering, Harbin Institute of Technology, 73 Huanghe Rd Nangang District, Harbin 150090, China
e-mail: yijunyan@hit.edu.cn

Z. Pei
Harbin Quan Traffic Technology Co., Ltd, Harbin 150090, Heilongjiang Province, China

M. Xu
Shenzhen Tianjian (Group) Co., Ltd, Shenzhen 518034, Guangdong Province, China

J. Cao · W. Hu · J. Ren
Liaoning Provincial Transportation Investment Group Co., Ltd, Shenyang 110166, Liaoning Province, China

R. Jing
Pavement Engineering, Delft University of Technology, Delft, The Netherlands

Published online: 09 December 2022

1 Introduction

Asphalt pavement is the most widely used pavement type for high-grade highways in various countries. However, in production and use, asphalt binder is inevitably impacted by light, heat, water, and other environmental factors, which can degrade its performance, weaken the adhesion between asphalt and aggregate and cause pits and cracks and other distress [1, 2]. These pavement distresses also seriously affect the driving comfort and durability of roads. Therefore,

researchers have notably researched the aging mechanism of asphalt.

The aging process of asphalt can be divided into two stages. The first stage involves the short-term aging caused by material production and mixture paving, and the second stage involves long-term aging during service. These two processes are mainly thermo-oxidative aging processes [3, 4]. However, ultraviolet (UV) aging inevitably affects the asphalt on the pavement surface [5]. Among these processes, thermo-oxidative and UV aging of asphalt can cause a series of chemical changes, seriously affecting the asphalt service performance [6, 7]. The research team of Peterson began to study the thermo-oxidative aging phenomenon of asphalt as early as the 1970s [8]. Asphalt is a complex mixture composed of relatively high-molecular weight hydrocarbons and nonmetallic derivatives containing millions of molecules. Therefore, it is not easy to completely characterize the molecular structure, chemical formula, and oxidation products of asphalt. However, modern component detection technology and computer simulation technology have revealed that the main products in the thermo-oxidative aging process of asphalt include ketones, sulfoxides, and other functional groups [9, 10]. The hardening mechanism of asphalt after oxidation is mainly caused by the strong molecular force between polar molecules and oxygen-containing functional groups in asphalt [11]. UV aging of asphalt only occurs within a few microns of the pavement surface, but it significantly impacts the asphalt performance. Generally, the energy value of ultraviolet light is higher than that needed to break the chemical bonds in asphalt molecular chains. Therefore, the breaking speed of molecular chains in asphalt is accelerated after irradiation by ultraviolet light, resulting in a free radical chain reaction. Although the depth of the UV aging effect is very shallow, the performance of asphalt on the pavement surface seriously declines, which can aggravate aggregate detachment and crack generation and can accelerate the damage process of the pavement structure [12–14].

Thermo-oxidative aging of asphalt mainly leads to the volatilization of components and chemical changes, eventually changing the asphalt composition. According to the properties of each component in asphalt, asphalt can be divided into four segments: saturates, aromatics, resins, and asphaltenes [15]. The proportions between these components correspond to different asphalt properties. The oxidation of asphalt components leads to the transformation of lightweight components into heavy components, while the volatilization of lightweight components can further increase the content of heavy components [16, 17]. In the oxidative aging process of asphalt, the relative content of saturates remains basically unchanged, while the aromatics undergo oxidation reactions to become asphaltenes or resins, resulting in a decrease in the aromatic content and an increase in the asphaltene content. In addition, in the mixing process, the heating temperature of the aggregate is often close to 200 °C. When hot aggregate comes into contact with the asphalt, the aromatic components in asphalt are also rapidly volatilized [18]. With increasing aging, the content of each component in asphalt gradually changes, and the structure of asphalt colloids is also altered. The increase in oxygen-containing functional groups leads to an increase in the content of polar components, the asphaltene aggregation effect, and the destruction of the stable structure of asphalt colloids, which worsens the properties of asphalt materials [19–21]. The results show that the penetration, ductility, and softening point of asphalt after aging strongly correlate with the asphalt component content change. The viscosity index exhibits the highest correlation with aging time. The phase angle is a suitable parameter to evaluate the aging degree [22, 23]. Studies have also confirmed the corresponding relationship between the change in functional groups and the rheological properties of specific asphalt types after thermo-oxidative aging, showing a strong linear correlation [24, 25]. However, different test methods yield different results for the fatigue performance of aged asphalt. Based on the stress or strain sweep test method, it was concluded that the fatigue life of asphalt increases after aging. The relaxation test method determined that the fatigue life of asphalt is attenuated after aging [26].

UV aging of asphalt mainly depends on ultraviolet radiation A (UVA, 320–400 nm) and ultraviolet radiation B (UVB, 280–320 nm) in sunlight. Asphalt exhibits different sensitivities to different wavelengths of ultraviolet light [27]. Under the same aging conditions, ultraviolet radiation within the range of 350–370 nm exerts the most severe impact on asphalt aging, followed by ultraviolet radiation within the ranges of 340–380 nm and 200–400 nm [28]. Within 0–24 h from the beginning of UV aging, the asphalt

aging depth rapidly increases, and the growth trend conforms to the power exponential growth model. When UV aging continues for more than 24 h, the aging depth of asphalt gradually tends to stabilize, which agrees more with the linear model [29, 30]. After UV aging, white powder products, rigid films, and local cracks are formed on the asphalt surface. The microhardness and elastic modulus of the asphalt surface rapidly increase [31, 32]. Moreover, adding short-chain alkanes or multibranched long-chain alkanes can inhibit the UV aging effect and improve the crack resistance of asphalt [33].

The aging effect of modified asphalt mainly includes oxidation aging of asphalt components and aged degradation of modifier materials [34, 35]. Generally, after short-term aging, polymer modifiers are notably degraded and eventually exhibit a medium-sized molecular structure. As a result, the performance of modified asphalt is reduced, but the aged asphalt can still maintain a particular modification effect. After long-term aging, almost all of the polymer modifiers have been degraded, and their modification effect has been lost [36, 37]. Therefore, modified asphalt's long-term aging performance is equivalent to that of ordinary aged asphalt, and negligible chemical reactions occur between the asphalt and the modifier [38–40]. Therefore, the study of the aging mechanism of base asphalt has a fundamental significance for analyzing asphalt performance changes. Researchers have also conducted much research work in this area. However, there are many sources of asphalt, and asphalt can be divided into different grades according to its performance characteristics. There are few studies on the change in the microstructure of asphalt materials considering different oil sources and grades under different aging conditions.

Research on the aging mechanism of asphalt has been widely performed. However, the aging characteristics of asphalt from the perspective of different oil sources and grades under different conditions have yet to be thoroughly analyzed. Moreover, the aging degree of different asphalt types remains to be determined. Therefore, this paper selected the seven kinds of asphalt most commonly used in China, created UV and thermo-oxidative aging conditions in homemade UV aging equipment and pressurized aging vessel (PAV) tests, respectively, and analyzed the influence of different oil sources, grades, and fillers on the microcharacteristics of aged asphalt based on nuclear magnetic resonance (NMR) ^{1}H spectra, attenuated total reflectance fourier transformation infrared spectroscopy (ATR-FTIR) spectra, and thermogravimetric test data. The composition changes in different asphalt materials under different aging conditions can be more deeply understood through the research in this paper. It is hoped that the study could provide a technical reference for proposing pavement maintenance schemes and enhancing pavement durability.

2 Materials

2.1 Asphalt binder

The study objective is to systematically analyze the aging characteristics of different asphalt types under different aging conditions. Seven asphalt types derived from four oil sources were selected for analysis, combined with the commonly used asphalt types in various regions of China. The specific asphalt conditions are listed in Table 1.

2.2 Filler

Among all aggregates of asphalt mixtures, the specific surface area of fillers is the largest, and asphalt mortar consisting of filler and asphalt exerts a notable impact on the performance of asphalt mixtures. Therefore, different kinds of fillers were selected to prepare asphalt mortar with a mass ratio of asphalt to filler of 1:1. Furthermore, the influence of fillers on the aging performance of asphalt under different aging conditions was explored. The three fillers selected in this study were obtained by grinding rocks. Their particle size range is summarized in Table 2.

3 Testing methods

The aging process of asphalt during service mainly involves thermo-oxidative and UV aging. Generally, the rolling thin-film oven test (RTFOT) is used to characterize the short-term aging process of asphalt during mixing and paving, and the PAV test method is used to characterize the long-term aging process of asphalt during service[41, 42]. However, due to the high temperature during mixing and paving, light

Table 1 Asphalt applied in this research

Type of asphalt	Abbreviation	Oil source	Application
Gao Fu (50#/70#/90#)	GF	Venezuelan heavy crude, onshore oilfields	South and Southeast China
SK (70#/90#)	SK	South Korea SK asphalt plant, Middle East oil source, onshore oilfield	Central and midwestern regions of China
An Da (90#)	AD	Production in Panjin, China, Liaohe oilfield, onshore Source	Northern China
Zhen Hai (70#)	ZH	Production at the Zhenhai Refinery Plant in Ningbo, China, offshore oilfield	Central and eastern regions of China

50 #, 70 # and 90 # are the median of asphalt penetration and represent different grades of asphalt

Table 2 Gradation of the fillers

Type	Particle size (mm)	Sieve residue (%)
Jinshan limestone filler (JS)	0.3	4.1
	0.15	11.7
	0.075 and below	84.2
Lishu limestone filler (LS)	0.3	1.0
	0.15	4.2
	0.075 and below	94.8
Basalt special filler (BS)	0.15	0
	0.075 and below	100

components of asphalt are volatilized. Therefore, the thermogravimetric test method was also employed in this study to explore the component volatilization degree of the different asphalt types during thermal aging. Furthermore, homemade ultraviolet-accelerated aging equipment was used to conduct asphalt UV aging tests [31]. The microstructure and composition of aged asphalt vary, and the material macroproperties are determined by the microproperties. Therefore, this study relied on the ATR-FTIR and NMR ^{1}H test methods to analyze the microscopic characteristics of the different asphalt types under different conditions.

3.1 Thermo-oxidative aging test of asphalt

Thermo-oxidative aging of asphalt mainly refers to the AASHTO T240 and AASHTO R28 specifications [41, 42]. First, the RTFOT test of asphalt (163 °C, 85 min) was conducted to simulate the aging stage during the construction phase. Then the RTFOT aged samples were subjected to the PAV aging test (100 °C, 2.1 MPa, 20 h) to characterize the long-term aging process of asphalt during service. Seven kinds of asphalt after PAV aging were used as thermo-oxidative aging test samples.

3.2 Thermogravimetric test of asphalt

The thermogravimetric test (TG) method can evaluate the change in the sample quality under specific temperature changes. This method is widely used in thermal stability and component analysis studies of materials. In this study, a synchronous thermal analysis infrared gas chromatography instrument of PerkinElmer company was used for TG analysis. When preparing the samples, the asphalt was firstly kept at 0 °C for 2 h, and the tweezers and scrapers were used to take a small number of samples. The sample mass was approximately 10 mg, and the sensitivity of the balance was 0.1 μg. The test mainly evaluated the volatilization characteristics of the different asphalt types under heating conditions. To eliminate the mass increase effect caused by oxidation, the test was performed in a nitrogen environment. In the test, the instrument temperature was increased

to 160 °C within half an hour, and a constant temperature was maintained for 2 h.

3.3 UV aging test of asphalt

Ultraviolet radiation is the critical factor driving the photooxidation aging process of asphalt, and selecting an ultraviolet light source is essential. Since the spectral distribution of Philips UVA fluorescent tubes is very close to that of the ultraviolet region of sunlight, a series of these tubes were selected as UV aging equipment in this study. The test temperature was 65 °C, close to the maximum temperature of the road surface in summer [31]. Considering that ultraviolet light may accelerate the oxidation reaction of asphalt, the ventilation system was opened to ensure sufficient oxygen. The preparation method of the asphalt sample for the UV aging test is consistent with that of the PAV test in AASHTO R28. During the test, the average irradiation intensity of the UV lamp is 102.3 W/m^2, and the distance between the sample's surface and the lamp is 8 cm. The total test time is 960 h, equivalent to 3–5 years of in-service aging in the field in Heilongjiang Province, China.

3.4 Attenuated total reflectance Fourier transformation infrared spectroscopy test

Attenuated total reflectance Fourier transformation infrared spectroscopy (ATR-FTIR) is based on the total reflection characteristics of a unique prism, in which a light beam is reflected multiple times on the surface of the test piece. Therefore, this technique can not only be used to measure elastic or viscous samples that are not easy to dissolve or melt and are difficult to crush but can also improve the test accuracy. The typical absorption peak of the infrared spectrum of asphalt is shown in Fig. 1.

As the asphalt binder generated no evident characteristic fingerprint within the wavenumber range of 1800–2400 cm^{-1}, the absorption peak within this range was not reflected in the spectrum. According to previous research results, the carbonyl index and sulfoxide index were used as evaluation indices of the aging degree of asphalt samples [43–45]. The carbonyl index and sulfoxide index can be calculated with Eqs. (1)–(3).

$$\text{Sulfoxide Index (SI)} = \frac{A_{1030}}{\sum A} \tag{1}$$

$$\text{Carbonyl Index (CI)} = \frac{A_{1700}}{\sum A} \tag{2}$$

$$\sum A = A_{(2924,2855)} + A_{1700} + A_{1600} + A_{1460} + A_{1378} + A_{1030} + A_{864} + A_{812} + A_{748} + A_{726} \tag{3}$$

3.5 Nuclear magnetic resonance ^{1}H spectrum test

The nuclear magnetic resonance hydrogen spectroscopy (^{1}H-NMR) technique is an effective means to analyze the distribution and content of hydrogen atoms in different structures of molecules. In the spectrum, the position of the peak represents the hydrogen atom position, and the area of the peak represents the hydrogen atom content. The change in molecular structure can be further analyzed by determining the distribution and content of hydrogen atoms. In this study, the AVANCEIIIHD 500 MHz NMR spectrometer of Bruker company was used for the test. Considering the dissolution characteristics of

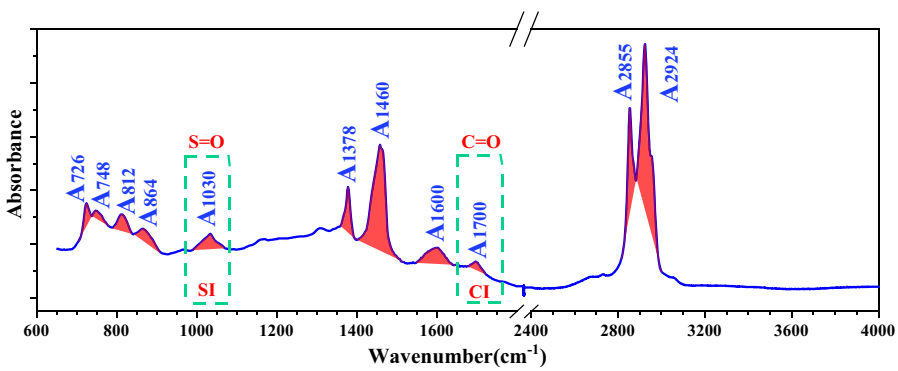

Fig. 1 Infrared spectrum of asphalt

asphalt, special deuterated chloroform was selected as the test solvent. Deuterated chloroform solvent usually contains a small amount (usually 0.1%) of tetramethylsilane (TMS) or chloroform ($CHCl_3$) for the calibration of chemical shifts. The ^1H NMR chemical shift in asphalt and its attribution are provided in Table 3 [46, 47]. Considering that the metal components in the filler can adversely affect or even damage the normal operation of the NMR spectrometer, ^1H spectrum scanning of asphalt mortar mixed with filler was not conducted in the study.

4 Results and discussion

4.1 Results of thermo-oxidative aging

4.1.1 Influence of the asphalt oil source on thermo-oxidative aging

(1) The changing trend of SI and CI indexes

The asphalt types with the same grade but different oil sources, as listed in Table 1, were selected to study the microscopic aging characteristics. The influence of thermo-oxidative aging on the microproperties of asphalt derived from various oil sources was analyzed via ATR-FTIR. Two control groups were set for asphalt derived from the different oil sources. AD90#, GF 90#, and SK90# comprised one control group, and ZH70#, GF70#, and SK70# comprised the other group. Infrared spectral analysis was performed of virgin asphalt and PAV-aged asphalt samples, with at least three parallel tests for each sample, and the results are the average value of the three tests. SI and CI of the different asphalt types were calculated according to Eqs. (1)–(3). The changes in the infrared spectra and functional group indices of the asphalt types derived from the different oil sources are shown in Fig. 2.

According to aging theory, the main products of aged asphalt include sulfoxide and ketone. The absorption band of sulfoxide occurs near 1030 cm^{-1}, and that of ketone occurs near 1700 cm^{-1}. In regard to 90# asphalt, the sulfoxide absorption band of GF90# changed the most obviously after aging, and the SI value increased by 8.4 times. The change in the SI value of SK90# was the smallest, increasing by 1.1 times. However, the SI value of AD90# before aging was also considerable. As sulfoxide is the main product during the rapid reaction period, it may be that the asphalt had aged to a certain extent during long-term storage or molding of the test piece. The change in the ketone content in SK90# after aging was the largest, and the CI value increased by 12.9 times. The CI value of GF90# exhibited the slightest change and increased by 3.7 times after aging. The changes in the functional groups of 90# asphalt with the same grade but different oil sources obviously differed after thermal-oxidative aging.

Figure 2 shows that in regard to 70# asphalt, the change degree of the SI value of GF70# was the highest after aging, increasing by 8.7 times. The SI change degree of ZH70# was the lowest, which increased by 1.1 times after aging. However, the SI value of ZH70# before aging was also high, so it may be that some asphalt aging occurred during long-term storage or molding of the test piece. The CI value of SK70# increased by 11.3 times after aging, and this change was the most obvious. The CI change in ZH70# was the smallest, and the value increased by 2.4 times. From the perspective of the aging index, the ZH70# asphalt provided the highest resistance to thermo-oxidative aging.

Table 3 Chemical shifts and attributions of the ^1H NMR spectrum [46, 47]

Types of H atoms	Chemical shift δ (ppm)	Positional attribution of the H atom
H_α	2.0–4.0	Hydrogen on the carbon atom of the α-position alkyl substituent on the aromatic ring
H_β	1.0–2.0	Saturated alkane hydrogen and hydrogen on aromatic ring β-alkyl substituent carbon
H_γ	0.5–1.0	Hydrogen on the carbon atom at the γ-position or more distant substitution position of the aromatic ring
H_{ar}	6.0–9.0	Hydrogen attached to an aromatic ring

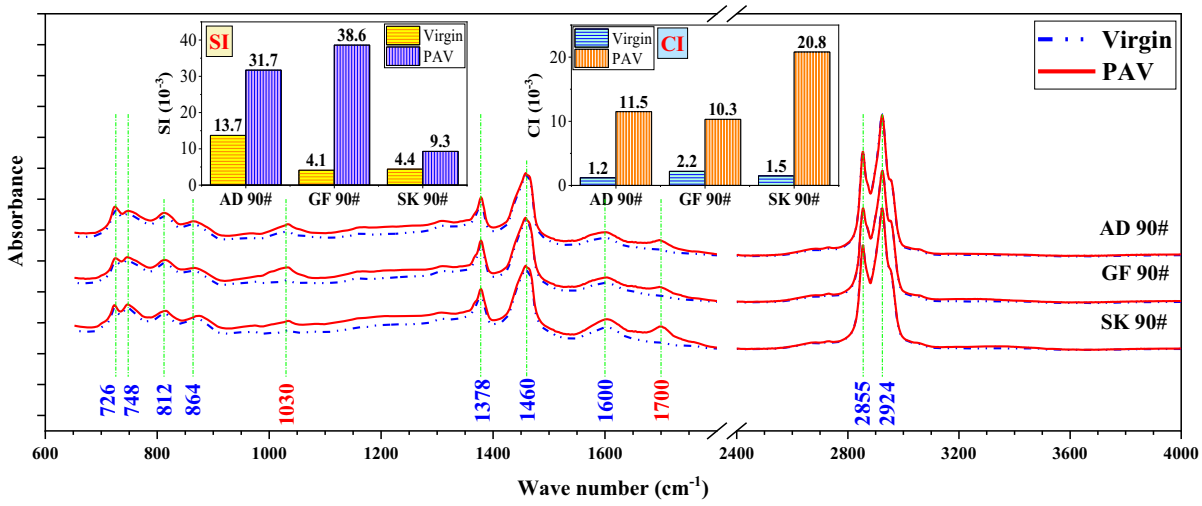

(a) Infrared spectra of the 90# asphalt specimens

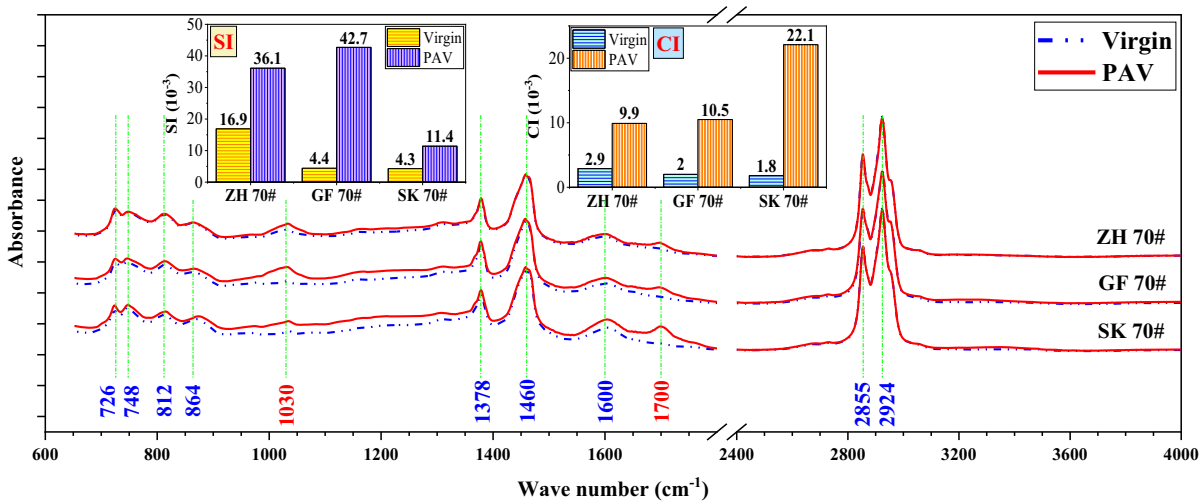

(b) Infrared spectra of the 70# asphalt specimens

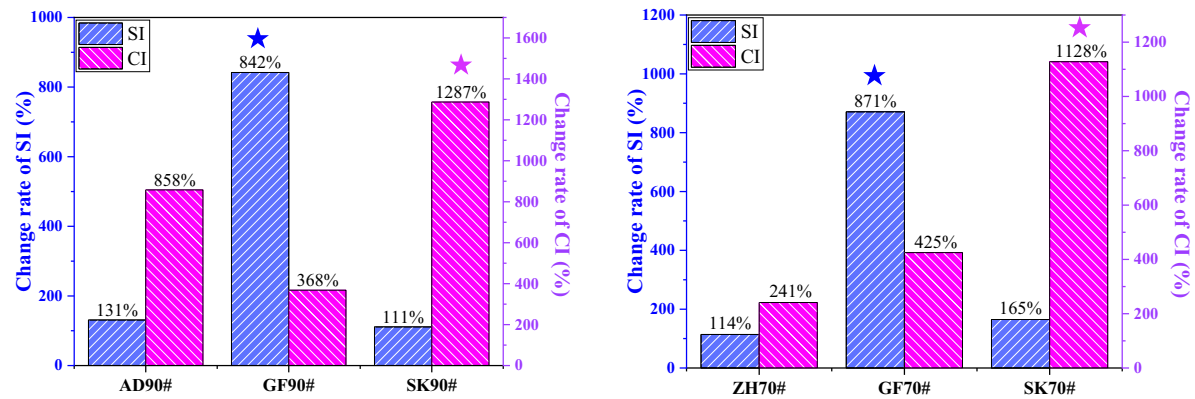

(c) Index change in the 90# asphalt specimens

(d) Index change in the 70# asphalt specimens

Fig. 2 Comparison of the infrared spectra of the asphalt specimens derived from the different oil sources (PAV)

The increase of carbonyl, sulfoxide, and other oxygen-containing functional groups after aging of asphalt leads to a significant increase in the polarity of asphalt molecules, the intermolecular force and the intermolecular aggregation. As a result, the intermolecular micelles of asphalt become more and larger, and the fluidity of asphalt becomes worse.

(2) Changes in the types of hydrogen atoms

The NMR test can distinguish the chemical environment of hydrogen atoms in asphalt. According to the chemical shift and the area of the peak in the spectrogram, the types and contents of hydrogen atoms can be obtained. Based on this method, we could analyze the changing trend of the asphalt microstructure under different aging conditions. Two control groups were established for asphalt obtained from various oil sources, which is consistent with the setting method of the ATR-FTIR tests. In addition, ^{1}H-NMR tests were performed on virgin and PAV-aged asphalt specimens. The ^{1}H-NMR test results for the asphalt specimens derived from the different oil sources are listed in Table 4.

After thermo-oxidative aging, the changing trends of H_{ar} and H_{α} of the different 90# asphalt specimens were different, but the content of H_{β} increased after aging, and the change range of GF90# was the largest. In contrast, the content of H_{γ} decreased after aging. Overall, the content of $H_{\beta} + H_{\gamma}$ increased after aging, indicating that the relative content of hydrogen atoms in the side chains of asphalt molecules increased after thermo-oxidative aging. Among the specimens, the hydrogen atom type of GF90# asphalt changed most significantly after thermo-oxidative aging, while the changing trend of SK90# was the lowest.

The contents of H_{ar} and H_{α} in 70# asphalt decreased after thermo-oxidative aging, indicating that the condensation dehydrogenation reaction occurred in the aromatic structure of asphalt during aging. However, the content of H_{β} increased after aging, and the changing trend of H_{γ} was not consistent. Moreover, the content of $H_{\beta} + H_{\gamma}$ increased after aging, indicating that the relative content of hydrogen atoms in the side chain of asphalt molecules increased after thermo-oxidative aging. The hydrogen atom content in GF70# changed most significantly after aging, and the trend of ZH70# was the lowest. The increase of H_{β} and $H_{\beta} + H_{\gamma}$ of asphalt thermal-oxidative aging products indicates that the fat-side chain length increases during the aging process, which leads to more internal friction when asphalt molecules move. Therefore, compared with the virgin sample, the aged asphalt needs a higher temperature to have the same relative displacement. Thus, the viscosity and softening point of asphalt will increase after aging [48–50].

4.1.2 *Influence of the asphalt grade on thermo-oxidative aging*

(1) The changing trend of SI and CI indexes

Asphalt specimens with the same oil source but different grades were selected for grouping. GF50#, GF70#, and GF90# comprised one control group, and SK70# and SK90# comprised the other group. ATR-FTIR tests of virgin and PAV-aged asphalt specimens were conducted, and CI and SI values were calculated according to Eqs. (1)–(3). The changes in the infrared spectra and the functional group indices of the asphalt specimens of different grades are shown in Fig. 3.

Table 4 Comparison of the ^{1}H NMR spectra of the asphalt specimens derived from the different oil sources (PAV)

Types of H atoms	AD 90#		GF 90#		SK 90#		ZH 70#		GF 70#		SK 70#	
	Virgin	PAV	Virgin	PAV	Virgin	PAV	Virgin	PAV	Virgin	PAV	Virgin	PAV
H_{ar}	0.8	0.5	1.1	2.3	12.1	5.1	11.1	10.5	18.9	8.6	1.4	0.4
H_{α}	12.5	3.4	17.2	1.5	3.2	9.9	13.1	4.8	17.7	9.9	7.8	3.6
H_{β}	65.5	79.8	54.9	71.1	64.7	67.0	34.5	40.3	53.3	69.6	56.9	79.7
H_{γ}	21.2	16.3	26.7	25.1	20.0	18.1	41.3	44.4	10.2	12.0	33.9	16.3
$H_{\beta} + H_{\gamma}$	86.7	96.1	81.6	96.2	84.7	85.1	75.8	84.7	63.5	81.6	90.8	96.0

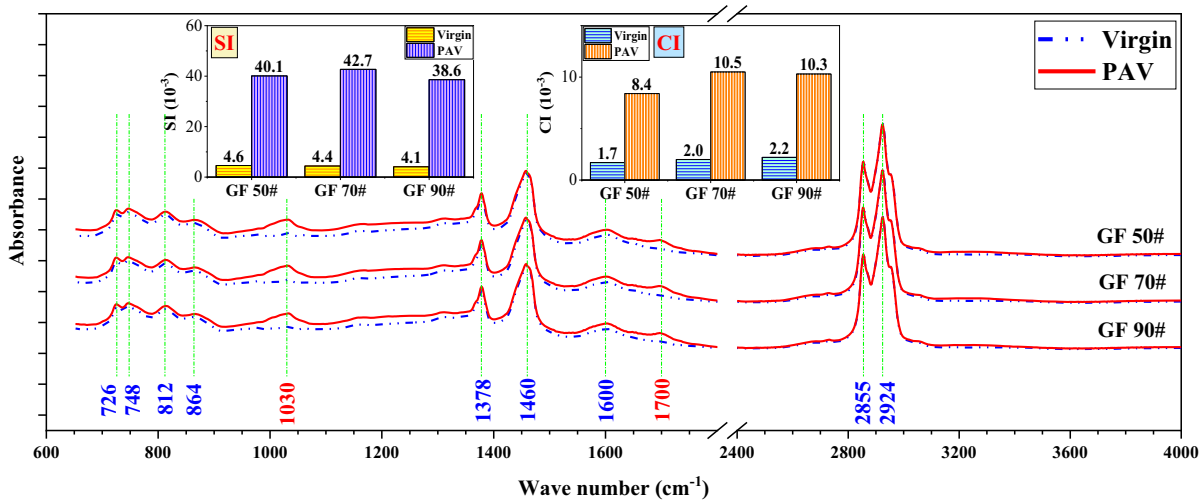

(a) Infrared spectra of the GF asphalt specimens

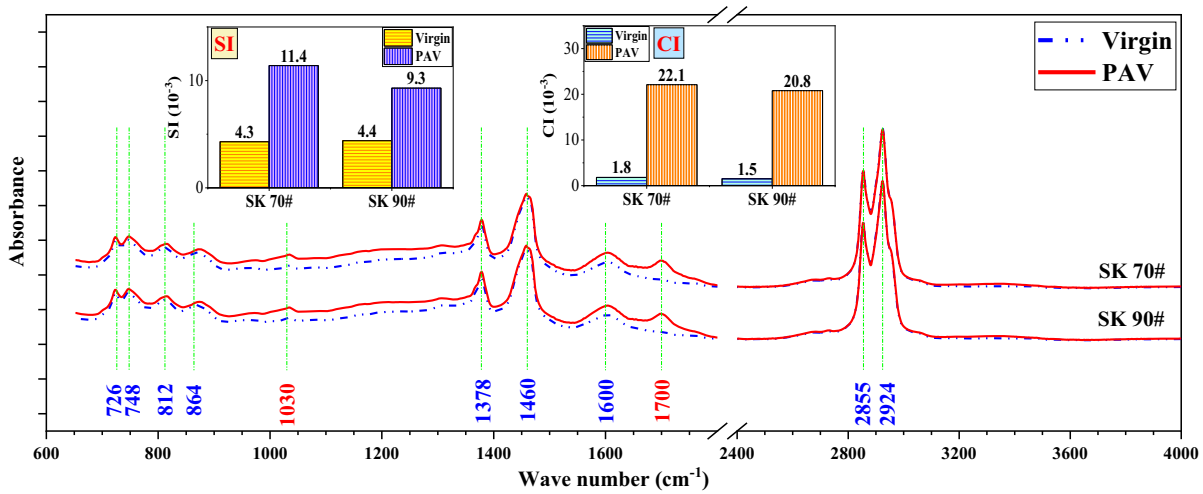

(b) Infrared spectra of the SK asphalt specimens

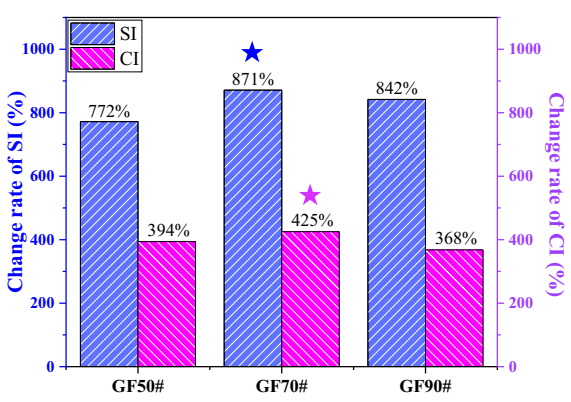

(c) Index change in the GF asphalt specimens

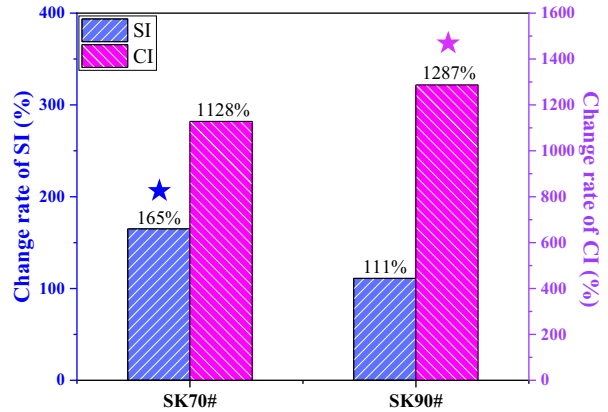

(d) Index change in the SK asphalt specimens

Fig. 3 Comparison of the infrared spectra of the asphalt specimens of the different grades (PAV)

Among the three kinds of GF asphalt specimens with different grades, the changing trend of the functional groups of the asphalt specimens after thermo-oxidative aging was very similar. In addition, the CI and SI values showed similar changes. This indicates that among the GF asphalt specimens with the same oil source, the grade change slightly affected the thermal-oxidative aging process of asphalt.

The changing trend and range of the infrared spectral curves of asphalt after thermo-oxidative aging were also very close between the two kinds of SK asphalt specimens with different grades. This shows that for the SK asphalt specimens with the same oil source, the influence of the grade on thermal-oxidative aging was relatively limited. According to the research results in the previous section, the effect of the asphalt oil source on the thermo-oxidative aging process was much more significant than that of the asphalt grade. The grade of the asphalt specimens produced from the same oil source slightly affected the thermal-oxidative aging results.

It can be seen from Fig. 3c, d that the sulfoxide group of GF asphalt increases significantly during aging, while the carbonyl group of SK asphalt increases significantly. Therefore, in the anti-aging design of asphalt binders, different inhibition schemes can be proposed according to the types of asphalt.

(2) Changes in the types of hydrogen atoms

Regarding asphalt with the same oil source, the influence of the asphalt grade on the change in hydrogen atoms after thermo-oxidative aging was explored. GF50#, GF70#, and GF90# were set as one control group, and SK70# and SK90# were set as another group. The ^{1}H-NMR hydrogen atom distribution in the asphalt specimens before and after aging is provided in Table 5.

The variation in the hydrogen atoms in GF50# was the lowest after aging, and the variation in the hydrogen atoms in GF90# was the highest after aging. Among the three GF asphalt specimens, no change rule for H_{ar} and H_{γ} could be determined before and after aging. However, the content of H_{α} decreased after thermo-oxidative aging, indicating that the α-carbon content in the aromatic structure of the GF asphalt specimens decreased after aging. In contrast, the contents of H_{β} and $H_{\beta} + H_{\gamma}$ increased after aging, indicating that the relative content of hydrogen atoms in the fat side chain of the asphalt molecules increased after aging. In general, the hydrogen atom slightly changed with the asphalt grade.

After aging, the H_{ar} content in the two kinds of SK asphalt decreased, indicating that condensation dehydrogenation occurred in the aromatic structure of these asphalt specimens during aging. In contrast, the contents of H_{β} and $H_{\beta} + H_{\gamma}$ increased after thermo-oxidative aging, showing that the relative content of hydrogen atoms in the side chain of the asphalt molecules increased after aging. However, the relative degree of hydrogen atom change in SK70# was higher than in SK90#.

The oil source and grade of asphalt could significantly impact the hydrogen atom distribution in asphalt after thermo-oxidative aging. However, according to the results in Sect. 4.1.1, the effect of the asphalt oil source on the change in functional groups after thermo-oxidation was highly significant, whereas the impact of the asphalt grade was relatively limited.

Table 5 Comparison of the ^{1}H NMR spectra of the asphalt specimens of the different grades (PAV)

Types of H atoms	GF 50#		GF 70#		GF 90#		SK 70#		SK 90#	
	Virgin	PAV	Virgin	PAV	Virgin	PAV	Virgin	PAV	Virgin	PAV
H_{ar}	11.2	12.5	18.9	8.6	1.1	2.3	1.4	0.4	12.1	5.1
H_{α}	14.9	6.7	17.7	9.9	17.2	1.5	7.8	3.6	3.2	9.9
H_{β}	54.1	61.4	53.3	69.6	54.9	71.1	56.9	79.7	64.7	67.0
H_{γ}	19.8	19.5	10.2	12.0	26.7	25.1	33.9	16.3	20.0	18.1
$H_{\beta} + H_{\gamma}$	73.9	80.9	63.5	81.6	81.6	96.2	90.8	96.0	84.7	85.1

4.1.3 *Influence of fillers on the thermal-oxidative aging performance of asphalt*

Asphalt mortar is the primary source of cementation in asphalt mixtures, which is significant for the performance of asphalt mixtures. Therefore, the influence of different fillers on the aging performance of asphalt was studied. Choosing AD90# and three kinds of asphalt mortars as the control group, the effect of fillers on asphalt functional groups during thermal-oxidative aging was analyzed. As the filler is mainly composed of inorganic compounds, the infrared spectrum of the asphalt mortar mixed with filler greatly changes, so it is not appropriate to conduct quantitative analysis according to the absorption peak area in the spectrum. The infrared spectra of AD90# and corresponding asphalt mortars before and after aging are shown in Fig. 4. The infrared spectra of the three asphalt mortars showed higher and wider absorption peaks within the wave number ranges of 820–880 cm^{-1} and 1300–1500 cm^{-1}. These positions mainly included characteristic absorption peaks caused by the filler composition. Through PAV aging curve analysis, the addition of the different fillers slightly affected the thermo-oxidative aging performance of asphalt, showing that the interaction between filler and asphalt did not significantly impact the aging process of asphalt.

4.2 Component volatilization results of the thermogravimetric test

Asphalt will undergo aging during mixing and paving under high-temperature. However, at the same time, this could dramatically promote the volatilization of lightweight components in asphalt, causing a change in the asphalt component proportion and performance. Therefore, the influence of asphalt sources, asphalt grades, and filler types on the volatilization of light components in asphalt was analyzed via the TG test method. The results are shown in Fig. 5.

The results show that the volatilization amounts of the various asphalt types derived from different oil sources were significantly different. Among them, SK90# yielded the most considerable volatilization amount, and the mass loss in 2 h at 160 °C was approximately 4%. In contrast, AD90# exhibited the least volatilization, and the total volatilization amount reached around 0.2%. The volatilization amount of SK90# was 20 times that of AD90#, indicating a significant difference. This also could result in apparent differences in the change degree of the performance of these two asphalts after long-term service when only considering the volatilization of lightweight components. The volatilization amount could also differ among asphalt types with the same oil source but different grades. In regard to GF asphalt, the volatilization amount of GF70# was the largest, while that of GF50# was the smallest. However, the volatilization amount of the three GF asphalt

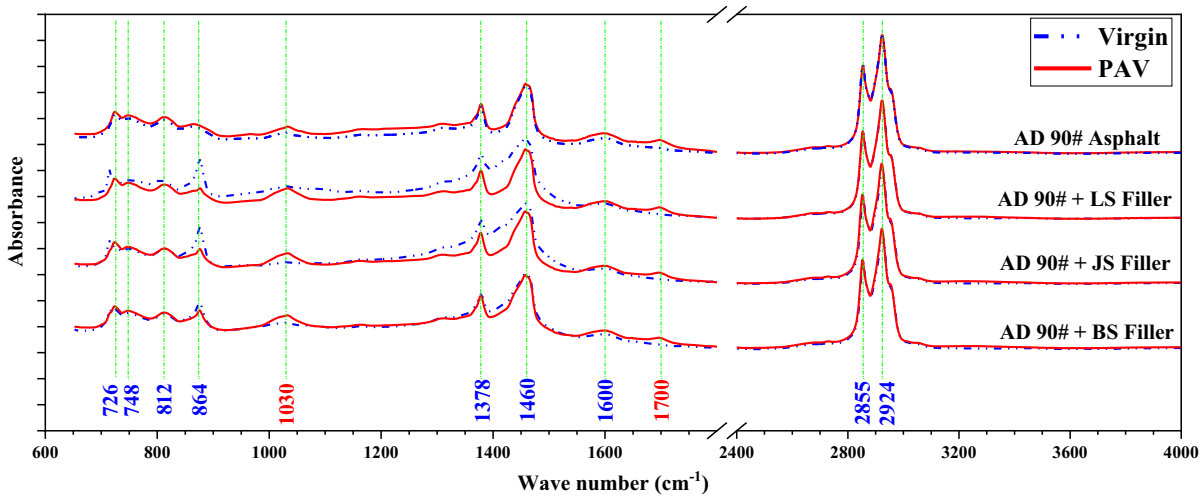

Fig. 4 Comparison of the infrared spectra of AD 90# asphalt with the different fillers (PAV)

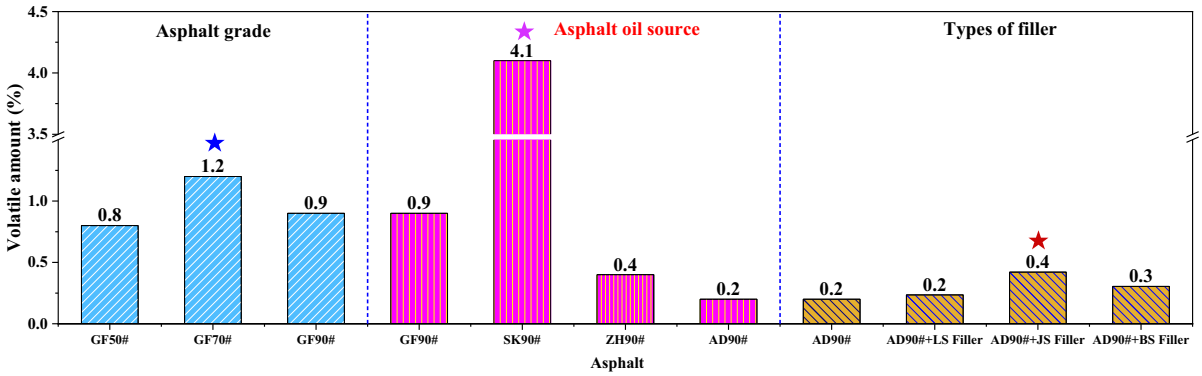

Fig. 5 Component volatilization results for the different types of asphalt

specimens ranged from 0.8 to 1.2%, and the range of the change degree was relatively small. It may be that the compositions of the asphalt specimens of the same oil source were generally similar. However, there were also differences in the composition between the asphalt specimens of the different grades, resulting in different volatilization effects. In addition, the volatilization-related change in the light components of asphalt after filler addition was limited, which was controlled at 0.2%, indicating that the filler slightly affected the volatility of the lightweight components in asphalt.

4.3 Results of UV aging

4.3.1 Influence of the asphalt oil source on UV aging

(1) The changing trend of SI and CI indexes

The mechanism of UV aging of asphalt is different from that of thermo-oxidative aging. Therefore, UV aging of asphalt derived from different oil sources was conducted, and the changes in the functional groups were analyzed via ATR-FTIR. AD90#, GF90#, and SK90# were set as the control group, and a 960-h UV aging test was performed with homemade equipment. The infrared spectra of asphalt before and after aging are shown in Fig. 6. Compared to the thermo-oxidative aging effect of asphalt described in Sect. 4.1.1, the infrared spectrum of asphalt after UV aging greatly changed. Compared to PAV aging, UV aging generated two new absorption peaks at approximately 1090 cm^{-1} and 3255 cm^{-1}. The absorption peak position of the alcohol group (C–OH) is near 1090 cm^{-1}, while the absorption peak position of hydrogen-bonded alcohol is near 3255 cm^{-1}. UV aging produced more alcohols in asphalt, which led to hydrogen bonding and intensified the aggregation between asphalt molecules. This also shows that the effect of UV aging on asphalt was more potent than that of thermo-oxidative aging. AD90# exhibited the most apparent change near 1090 cm^{-1}, indicating that it produced the most alcohol after UV aging. Therefore, the changing trend of the hydrogen bond absorption peak of AD90# near 3255 cm^{-1} was also the most notable. However, SK90# exhibited no significant change near 1090 cm^{-1}, so its hydrogen bond absorption peak generated a slight change trend near 3255 cm^{-1}. Regarding SI, the value of GF90# changed the most after UV aging, increasing by 2.6 times. The SI value of AD90# exhibited the slightest change, rising 8%. Regarding CI, AD90# showed the most apparent change after UV aging, with the value increasing 24.4 times. The CI value of GF90# changed slightly, rising by 5.8 times. The SI and CI values of SK90# varied between those of AD90# and GF90#.

(2) Changes in the types of hydrogen atoms

^{1}H-NMR tests were performed on virgin and UV-aged asphalt samples derived from three oil sources. The test results are provided in Table 6. After UV aging, the changing trends of H_{ar} and H_{α} of the different asphalt types were different. However, the content of H_{β} decreased after aging, which showed that cleavage of aliphatic branched chains occurred in the three asphalt specimens during UV aging. In

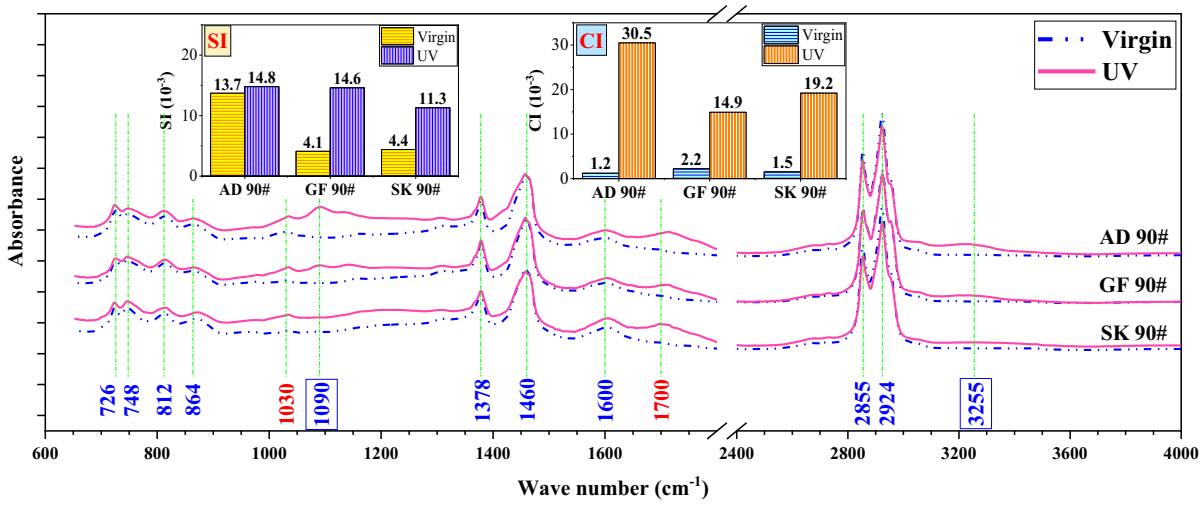

(a) Infrared spectra of the 90# asphalt samples

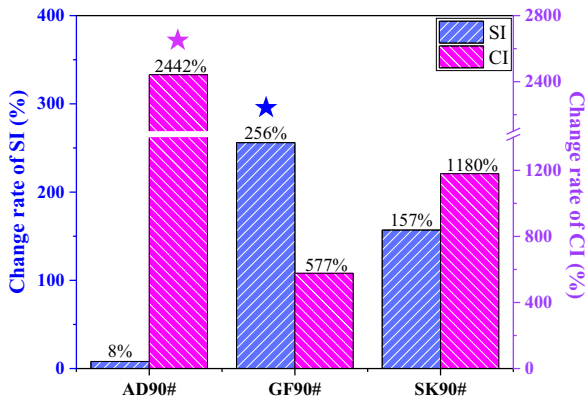

(b) Index change rate of SI and CI

Fig. 6 Comparison of the infrared spectra of the 90# asphalt samples derived from the different oil sources (UV)

Table 6 Comparison of the ^{1}H NMR spectra of the 90# asphalt specimens from the different oil sources (UV)

Types of H atoms	AD 90#		GF 90#		SK 90#	
	Virgin	UV	Virgin	UV	Virgin	UV
H_{ar}	0.8	2.7	1.1	1.6	12.1	11.4
H_{α}	12.5	11.4	17.2	4.7	3.2	7.9
H_{β}	65.5	46.4	54.9	53.0	64.7	53.9
H_{γ}	21.2	39.6	26.7	40.7	20.0	26.8
$H_{\beta} + H_{\gamma}$	86.7	86.0	81.6	93.7	84.7	80.7

addition, the change range of H_{β} of AD90# was the largest. On the other hand, the content of H_{γ} increased after aging, indicating that the content of alkyl substituents in the aromatic rings increased during UV aging. Moreover, the change range of H_{γ} in AD90# was the largest, and that of the SK90# asphalt specimen was the smallest. Overall, the change degree of the hydrogen atoms in SK90# after

UV aging was minimal. Compared to the thermo-oxidative aging effect of asphalt described in Sect. 4.1.1, the content change trends of H_β and H_γ were the opposite. The results showed that thermo-oxidative and UV aging of asphalt generated different effects, and the impact of UV aging was more notable.

4.3.2 *Influence of the asphalt grade on UV aging*

(1) The changing trend of SI and CI indexes

UV aging tests were carried out on asphalt samples with the same oil source but different grades. SK70# and SK90# samples were used as the control group. The infrared spectrum and functional group changes in the SK asphalt samples before and after aging are shown in Fig. 7. The changing trend and degree of the infrared spectrum after UV aging were relatively similar between the two kinds of SK asphalt samples with different grades. Regarding SI and CI, the change degree of SK70# after aging was slightly higher, indicating that the UV aging resistance of SK70# was lower than that of SK90#. Compared to the change shown in Fig. 3, UV aging of SK asphalt produced a more significant change than thermo-oxidative aging, indicating that the UV aging effect was more significant. From the perspective of the infrared spectrum change degree and the functional group growth trend, the asphalt oil source exerted a more significant effect on UV aging. In contrast, the asphalt grade slightly affected the UV aging process.

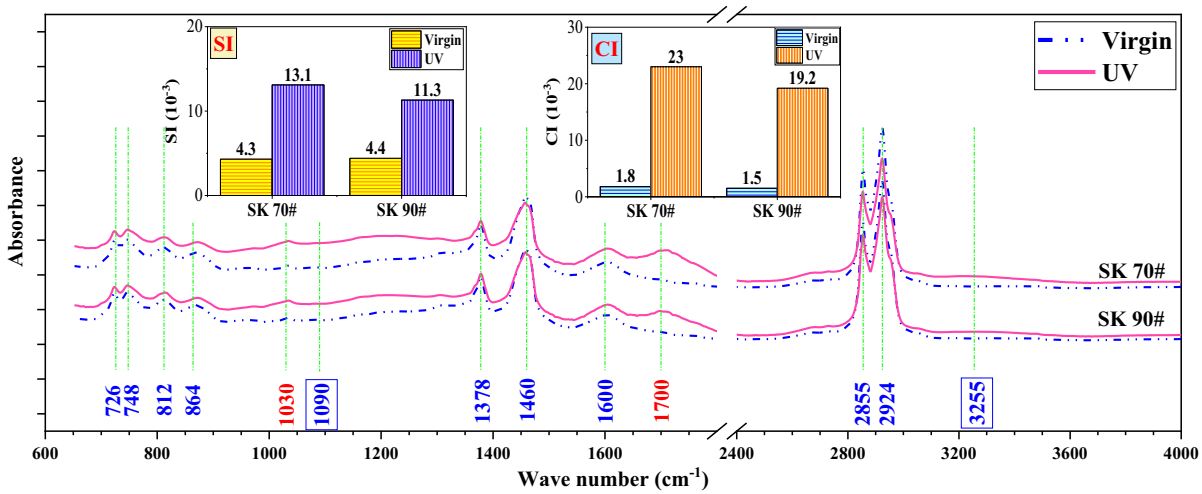

(a) Infrared spectra of the SK asphalt samples

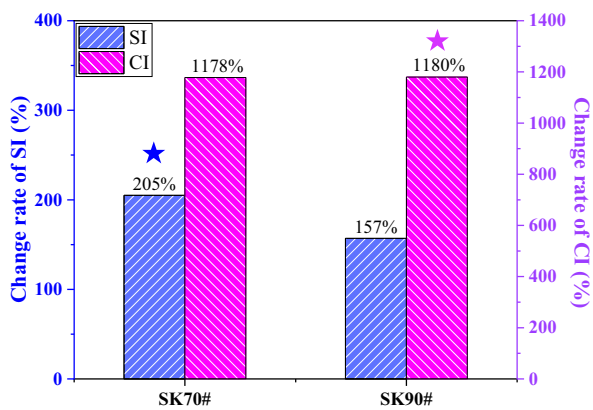

(b) Index change rate of SI and CI

Fig. 7 Comparison of the infrared spectra of the SK asphalt samples with the different grades (UV)

Table 7 Comparison of the ^{1}H NMR spectra of the SK asphalt samples of the different grades (UV)

Types of H atoms	SK 70#		SK 90#	
	Virgin	UV	Virgin	UV
H_{ar}	1.4	3.9	12.1	11.4
H_{α}	7.8	2.8	3.2	7.9
H_{β}	56.9	53.3	64.7	53.9
H_{γ}	33.9	40.0	20.0	26.8
$H_{\beta} + H_{\gamma}$	90.8	93.3	84.7	80.7

(2) Changes in the types of hydrogen atoms

The ^{1}H-NMR hydrogen atom distribution in the SK asphalt samples before and after UV aging is provided in Table 7. After UV aging, the change trends of H_{ar} and H_{α} of the SK asphalt samples were different, but the change trends of H_{β} and H_{γ} were the same. The content of H_{β} decreased after aging, which indicates that the SK asphalt samples experienced fat branch chain cracking during UV aging. The content of H_{γ} increased after aging, indicating that the content of γ-hydrogen in asphalt increased after UV aging, and the alkyl substituents on the aromatic rings of the asphalt molecules increased. The relative change degree of hydrogen atoms in SK90# after UV aging was higher than that of SK70#. Compared to the hydrogen atom distribution data for thermo-oxidative aging listed in Table 5, the change trends of the H_{β} and H_{γ} contents after UV aging were the opposite, which also shows that UV and thermo-oxidative aging yielded different effects on asphalt.

4.3.3 Influence of fillers on UV aging of asphalt

UV aging and ATR-FTIR tests were conducted involving AD90# and its asphalt mortars, and the results are shown in Fig. 8. After UV aging, the infrared spectral curves of the different asphalt mortars were almost the same, indicating that the addition of different fillers slightly affected the UV aging performance of asphalt. The result is also close to that of thermo-oxidative aging, showing that filler addition did not exert a significant impact on either thermo-oxidative or UV asphalt aging.

5 Conclusions

Based on thermo-oxidative and UV aging processes, this study systematically analyzed the influence of asphalt oil sources, asphalt grades, and fillers on the asphalt aging effect and microstructure change. For the seven asphalts in this paper, the conclusions are as follows:

(1) SI and CI can be used to evaluate the aging degree of asphalt quantitatively. Considering the aging resistance design, GF asphalt should pay more attention to the inhibition of sulfoxide generation, and SK asphalt should focus on the inhibition of carbonyl generation.

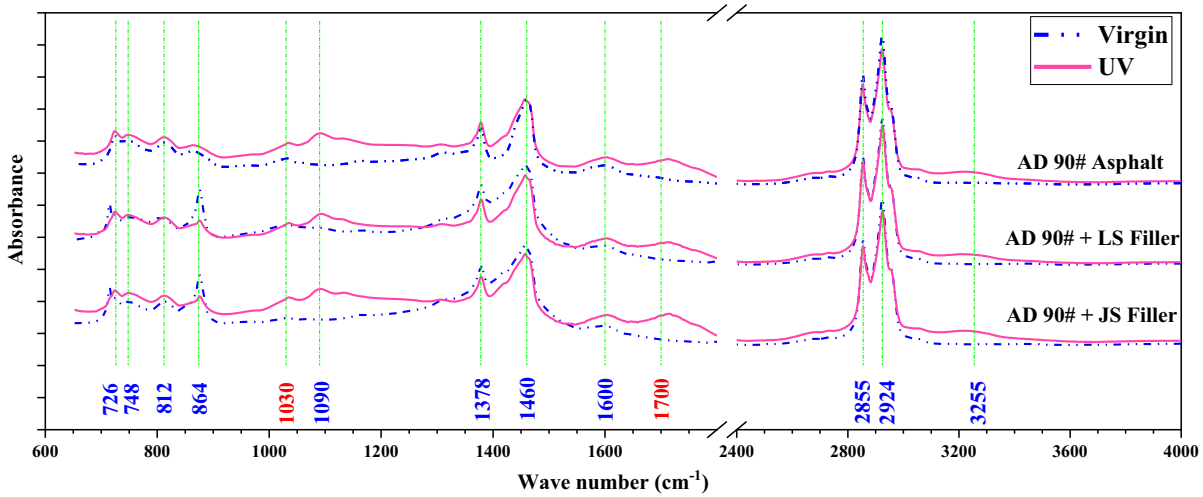

Fig. 8 Comparison of the infrared spectra of the AD 90# asphalt samples with the different fillers (UV)

(2) UV aging of asphalt will produce more alcohols or ethers and form more hydrogen bonds than thermo-oxidative aging. Therefore, in the design of resistance to UV aging, special consideration can be given to adding materials that inhibit the production of alcohols or ethers.
(3) The parameters H_β, H_γ, and $H_\beta + H_\gamma$ of ^{1}H-NMR can be used to evaluate the aging degree of asphalt qualitatively. After thermo-oxidative aging of asphalt, the fat-side chain length tends to increase. However, after UV aging, the fat-side chain undergoes a certain degree of cracking reaction, and the content of alkyl substituents on the aromatic ring tends to increase.
(4) The influence of oil sources on asphalt aging is most significant. When SK asphalt is used as the binder, the oil compensation design can be appropriately increased to reduce the impact of its volatilization effect. In addition, the interaction between the filler and asphalt slightly affects the aging mechanism of asphalt.

This study mainly focuses on analyzing the microcharacteristics of different asphalts under different aging conditions. The follow-up research will focus on the changing rules of the macroscopic properties of these asphalts after aging. The aging characteristics of different asphalts can be explained more comprehensively through the combination of micro-analysis and macro performance.

Acknowledgements This work was financially supported by the National Natural Sciences Foundation of China (Nos. 51878229, 52178420), China Postdoctoral Science Foundation (2021M702293), Science and technology project of the Ministry of Housing and Urban Rural Development (2019-K-137), Special subsidy from Heilongjiang Provincial People's Government (HITTY-20190028), Key R & D projects in Liaoning Province (2020JH210300097), Harbin Science and technology project (2019CYJBCG0192).

Author contributions Data curation: ZP, MX; Formal analysis: JY, ZP, MX; Investigation: ZP, WH, JR; Methodology: JY, DF, RJ; Project administration: JY, DF, JC; Resources: JY, JC, DF; Supervision: DF, JY; Writing – original draft: ZP, JY, MX.

Declarations

Conflict of interest The authors declare that they have no conflict of interest.

References

1. Oldham D, Qu X, Wang HN, Fini EH (2020) Investigating change of polydispersity and rheology of crude oil and bitumen due to asphaltene oxidation. Energy Fuels 34(8):10299–10305. https://doi.org/10.1021/acs.energyfuels.0c01344
2. Chen Z, Yi JY, Zhao H, Luan H, Xu M, Zhang LD, Feng DC (2021) Strength development and deterioration mechanisms of foamed asphalt cold recycled mixture based on MD simulation. Constr Buil Mater 269:121324. https://doi.org/10.1016/j.conbuildmat.2020.121324
3. Zhou T, Cao LP, Fini EH, Li LW, Liu ZY, Dong ZJ (2020) Behaviors of asphalt under certain aging levels and effects of rejuvenation. Constr Buil Mater 249:118748. https://doi.org/10.1016/j.conbuildmat.2020.118748
4. Hofko B, Porot L, Cannone AF, Poulikakos L, Huber L, Lu X, Mollenhauer K, Grothe H (2018) FTIR spectral analysis of bituminous binders: reproducibility and impact of ageing temperature. Mater Struct 51(2):45. https://doi.org/10.1617/s11527-018-1170-7
5. Zhou L, Zhang Y, Liu BY (2021) Aging characteristics of asphalt binder under strong ultraviolet irradiation in Northwest China. Sustainability 13(19):10753. https://doi.org/10.3390/su131910753
6. Hosseinnezhad S, Zadshir M, Yu XK, Yin HM, Sharma BK, Fini EH (2019) Differential effects of ultraviolet radiation and oxidative aging on bio-modified binders. Fuel 251:45–56. https://doi.org/10.1016/j.fuel.2019.04.029
7. Feng ZG, Bian HJ, Li XJ, Yu JY (2016) FTIR analysis of UV aging on bitumen and its fractions. Mater Struct 49:1381–1389. https://doi.org/10.1617/s11527-015-0583-9
8. Petersen JC, Barbour FA, Dorrence SM (1975) Identification of dicarboxylic anhydrides in oxidized asphalts. Anal Chem 47(1):107–111. https://doi.org/10.1021/ac60351a005
9. Petersen JC, Plancher H (1981) Quantitative determination of carboxylic acids and their salts and anhydrides in asphalts by selective chemical reactions and differential infrared spectrometry. Anal Chem 53(6):786–789. https://doi.org/10.1021/ac00229a010
10. Petersen JC, Glaser R (2011) Asphalt oxidation mechanisms and the role of oxidation products on age hardening revisited. Road Mater Pavement Des 12(4):795–819. https://doi.org/10.1080/14680629.2011.9713895
11. Pahlavan F, Hung AM, Zadshir M, Hosseinnezhad S, Fini EH (2018) Alteration of π-electron distribution to induce deagglomeration in oxidized polar aromatics and asphaltenes in an aged asphalt binder. ACS Sustain Chem Eng 6(5):6554–6569. https://doi.org/10.1021/acssuschemeng.8b00364
12. Alamdary YA, Singh S, Baaj H (2019) Laboratory simulation of the impact of solar radiation and moisture on long-term age conditioning of asphalt mixes. Road Mater Pavem Des 20(Suppl 1):S521–S532. https://doi.org/10.1080/14680629.2019.1587496
13. Hung A, Fini EH (2020) Surface morphology and chemical mapping of UV-aged thin films of bitumen. ACS Sustain Chem Eng 8(31):11764–11771. https://doi.org/10.1021/acssuschemeng.0c03877

14. Liu L, Liu ZH, Hong LL, Huang Y (2020) Effect of ultraviolet absorber (UV-531) on the properties of SBS-modified asphalt with different block ratios. Constr Buil Mater 234:117388. https://doi.org/10.1016/j.conbuildmat.2019.117388
15. Shi HQ, Xu T, Jiang RL (2017) Combustion mechanism of four components separated from asphalt binder. Fuel 192:18–26. https://doi.org/10.1016/j.fuel.2016.11.110
16. Xu M, Yi JY, Qi P, Wang H, Marasteanu M, Feng DC (2019) Improved chemical system for molecular simulations of asphalt. Energy Fuels 33:3187–3198. https://doi.org/10.1021/acs.energyfuels.9b00489
17. Bhasin A, Ganesan V (2017) Preliminary investigation of using a multi-component phase field model to evaluate microstructure of asphalt binders. Int J Pavem Eng 18(9):775–782. https://doi.org/10.1080/10298436.2015.1065998
18. Zupanick M, Baselice V (1997) Characterizing asphalt volatility. Transp Res Rec J Transp Res Board 1586:1–9. https://doi.org/10.3141/1586-01
19. Sharma A, Groenzin H, Tomita A, Mullins OC (2002) Probing order in asphaltenes and aromatic ring systems by HRTEM. Energy Fuels 16(2):490–496. https://doi.org/10.1021/ef010240f
20. Bao CH, Xu Y, Zheng CF, Nie L, Yang X (2022) Rejuvenation effect evaluation and mechanism analysis of rejuvenators on aged asphalt using molecular simulation. Mater Struct 55:52. https://doi.org/10.1617/s11527-022-01890-3
21. Guern ML, Chailleux E, Farcas F, Dreessen S, Mabille I (2010) Physico-chemical analysis of five hard bitumens: identification of chemical species and molecular organization before and after artificial aging. Fuel 89(11):3330–3339. https://doi.org/10.1016/j.fuel.2010.04.035
22. Wang F, Xiao Y, Cui PD, Lin JT, Li ML, Chen ZW (2020) Correlation of asphalt performance indicators and aging Degrees: a review. Constr Buil Mater 250:118824. https://doi.org/10.1016/j.conbuildmat.2020.118824
23. Puello J, Afanasjeva N, Alvarez M (2013) Thermal properties and chemical composition of bituminous materials exposed to accelerated ageing. Road Mater Pavem Des 14(2):278–288. https://doi.org/10.1080/14680629.2013.785799
24. Jing RX, Varveri A, Liu XY, Scarpas A, Erkens S (2021) Ageing effect on chemo-mechanics of bitumen. Road Mater Pavem Des 22(5):1044–1059. https://doi.org/10.1080/14680629.2019.1661275
25. Hou XD, Liang B, Xiao FP, Wang JY, Wang T (2020) Characterizing asphalt aging behaviors and rheological properties based on spectrophotometry. Constr Buil Mater 256:119401. https://doi.org/10.1016/j.conbuildmat.2020.119401
26. Jing RX, Varveri A, Liu XY, Scarpas A, Erkens S (2020) Rheological, fatigue and relaxation properties of aged bitumen. Inter J Pavem Eng 21(8):1024–1033. https://doi.org/10.1080/10298436.2019.1654609
27. Li YY, Wu SP, Liu QT, Dai Y, Li CM, Li HC, Nie S, Song W (2019) Aging degradation of asphalt binder by narrow-band UV radiations with a range of dominant wavelengths. Constr Buil Mater 220:637–650. https://doi.org/10.1016/j.conbuildmat.2019.06.035
28. Li YY, Wu SP, Liu QT, Xie J, Li HC, Dai Y, Li CM, Nie S, Song W (2019) Aging effects of ultraviolet lights with same dominant wavelength and different wavelength ranges on a hydrocarbon-based polymer (asphalt). Polym Test 75:64–75. https://doi.org/10.1016/j.polymertesting.2019.01.025
29. Zeng WB, Wu SP, Pang L, Chen HH, Hu JX, Sun YH, Chen ZW (2018) Research on Ultra Violet (UV) aging depth of asphalts. Constr Buil Mater 160:620–627. https://doi.org/10.1016/j.conbuildmat.2017.11.047
30. Li YY, Feng JL, Yang F, Wu SP, Liu QT, Bai T, Liu ZJ, Li CM, Gu DJ, Chen AQ, Jin YS (2021) Gradient aging behaviors of asphalt aged by ultraviolet lights with various intensities. Constr Buil Mater 295:123618. https://doi.org/10.1016/j.conbuildmat.2021.123618
31. Xu M, Yi JY, Pei ZS, Feng DC, Huang YD, Yang Y (2017) Generation and evolution mechanisms of pavement asphalt aging based on variations in surface structure and micromechanical characteristics with AFM. Mater Today Commun 12:106–118. https://doi.org/10.1016/j.mtcomm.2017.07.006
32. Chen ZH, Zhang HL, Duan HH (2020) Investigation of ultraviolet radiation aging gradient in asphalt binder. Constr Buil Mater 246:118501. https://doi.org/10.1016/j.conbuildmat.2020.118501
33. Hosseinnezhad S, Hung AM, Mousavi M, Sharma BK, Fini EH (2020) Resistance mechanisms of biomodified binders against ultraviolet exposure. ACS Sustain Chem Eng 8(6):2390–2398. https://doi.org/10.1021/acssuschemeng.9b05490
34. Sun L, Wang YY, Zhang YM (2014) Aging mechanism and effective recycling ratio of SBS modified asphalt. Constr Buil Mater 70:26–35. https://doi.org/10.1016/j.conbuildmat.2014.07.064
35. Wang FS, Zhang L, Zhang XS, Li HC, Wu SP (2020) Aging mechanism and rejuvenating possibility of SBS copolymers in asphalt binders. Polymers 12(1):92. https://doi.org/10.3390/polym12010092
36. Wang YY, Sun L, Qin YX (2015) Aging mechanism of SBS modified asphalt based on chemical reaction kinetics. Constr Buil Mater 91:47–56. https://doi.org/10.1016/j.conbuildmat.2015.05.014
37. Zhu CZ, Zhang HL, Zhang DM, Chen ZH (2018) Influence of base asphalt and SBS modifier on the weathering aging behaviors of sbs modified asphalt. J Mater Civ Eng 30(3):04017306. https://doi.org/10.1061/(ASCE)MT.1943-5533.0002188
38. Wei CW, Duan HH, Zhang HL, Chen ZH (2019) Influence of SBS modifier on aging behaviors of SBS-modified asphalt. J Mater Civ Eng 31(9):04019184. https://doi.org/10.1061/(ASCE)MT.1943-5533.0002832
39. Islam SS, Ransinchung GDRN, Singh B, Singh SK (2022) Effect of short-term and long-term ageing on the elastic and creep behaviour of modified binder containing different SBS copolymer. Mater Struct 55:144. https://doi.org/10.1617/s11527-022-01902-2
40. Zhang DM, Zhang HL, Shi CJ (2017) Investigation of aging performance of SBS modified asphalt with various aging methods. Constr Buil Mater 145:445–451. https://doi.org/10.1016/j.conbuildmat.2017.04.055

41. AASHTO (2013) Standard method of test for effect of heat and air on a moving film of asphalt binder (rolling thin-film oven test). AASHTO T 240–2013 Washington, DC
42. AASHTO (2012) Standard practice for accelerated aging of asphalt binder using a pressurized aging vessel (PAV). AASHTO R28–2012, Washington, DC
43. Lamontagne J, Dumas P, Mouillet V, Kister J (2001) Comparison by Fourier transform infrared (FTIR) spectroscopy of different ageing techniques: application to road bitumens. Fuel 80(4):483–488. https://doi.org/10.1016/S0016-2361(00)00121-6
44. Hofko B, Alavi MZ, Grothe H, Jones D, Harvey J (2017) Repeatability and sensitivity of FTIR ATR spectral analysis methods for bituminous binders. Mater Struct 50(3):187. https://doi.org/10.1617/s11527-017-1059-x
45. Jing RX, Liu XY, Varveri A, Scarpas A, Erkens S (2018) The effect of ageing on chemical and mechanical properties of asphalt mortar. Appl Sci 8(11):2231. https://doi.org/10.3390/app8112231
46. Christopher J, Sarpal AS, Kapur GS, Krishna A, Tyagi BR, Jain MC, Jain SK, Bhatnagar AK (1996) Chemical structure of bitumen-derived asphaltenes by nuclear magnetic resonance spectroscopy and X-ray diffractometry. Fuel 75(8):999–1008. https://doi.org/10.1016/0016-2361(96)00023-3
47. Li GN, Tan YQ (2022) The construction and application of asphalt molecular model based on the quantum chemistry calculation. Fuel 308:122307. https://doi.org/10.1016/j.fuel.2021.122037
48. Zhang MY, Hao PW, Dong S, Yuan GA (2020) Asphalt binder micro-characterization and testing approaches: a review. Constr Buil Mater 151:107255. https://doi.org/10.1016/j.measurement.2019.107255
49. Khiavi AK, Ghanbari A, Ahmadi E (2021) Evaluation of poly 2-hydroxyethyl methacrylate—modified bitumen aging using NMR and FTIR techniques. J Transp Eng B-Pave 147(1):04020087. https://doi.org/10.1061/JPEODX.0000228
50. Siddiqui MN (2009) NMR Fingerprinting of chemical changes in asphalt fractions on oxidation. Pet Sci Technol 27(17):2033–2045. https://doi.org/10.1080/10916460802668622